peptone broth supplemented with 0.1% glucose at 25°C with shaking at 100 rpm.
30. Animal studies were conducted in accordance with the NIH guidelines for the care and use of laboratory animals. We thank A. Jackson for assistance with preparation of TGase2, B. Taylor for assistance with the animal experiments, and C. M. Allen for histological assessments of infected mouse tissues. Support for this research was provided from grant 1 R01 DE11375-05A2 from the National Institute of Dental and Craniofacial Research (P.S.) and AI32556 from the National Institute for Allergy and Infectious Diseases (P.L.F.).

30 October 1998; accepted 3 February 1999

The Predictive Value of Changes in Effective Connectivity for Human Learning

C. Büchel,* J. T. Coull, K. J. Friston

During learning, neural responses decrease over repeated exposure to identical stimuli. This repetition suppression is thought to reflect a progressive optimization of neuronal responses elicited by the task. Functional magnetic resonance imaging was used to study the neural basis of associative learning of visual objects and their locations. As expected, activation in specialized cortical areas decreased with time. However, with path analysis it was shown that, in parallel to this adaptation, increases in effective connectivity occurred between distinct cortical systems specialized for spatial and object processing. The time course of these plastic changes was highly correlated with individual learning performance, suggesting that interactions between brain areas underlie associative learning.

Studies of associative learning aim (i) to identify neural structures that constitute memory systems and (ii) to characterize the network properties that comprise interactions among their components. The first aim has been addressed largely by using functional neuroimaging, on the basis of the principle of functional specialization. In the case of object-location memory, several functional studies have demonstrated activation of ventral occipital and temporal regions during the retrieval of object identity and, conversely, increased responses in dorsal parietal areas during the retrieval of spatial location (*1–3*). These results suggest domain-specific representations in posterior neocortical structures, closely related to those involved in perception, and they accord with the segregation of ventral and dorsal pathways in processing categorical or spatial stimulus features, respectively (*4*). Another phenomenon observed in some learning studies is a decrease of neural responses (that is, adaptation) to repeated stimulus presentations. This repetition suppression has been replicated consistently in primate electrophysiological and human functional imaging studies (*5*). Although certainly not the only electrophysiological correlate of learning, it is ubiquitous and a useful measure of learning-related changes intrinsic to unit or population responses. For object-location learning, it is intuitively likely that two specialized systems need to interact to establish an association. Domain-specific representations or repetition suppression is not sufficient to account for this associative component (*6*). In other words, functional segregation and localized response properties cannot account for associative learning alone. Here, we address the functional integration of different systems to characterize learning from a different perspective, namely, that of effective connectivity (*7*).

Whole-brain functional magnetic resonance imaging (fMRI) was used to test the hypotheses that (i) repeated stimulus presentation during learning will lead to adaptation of evoked cortical responses (repetition suppression) and (ii) learning the association of two stimulus attributes that are processed in segregated cortical regions is accompanied by changes in effective connectivity between these regions over time. We chose object location and object identity as the two attributes to be associated because they are processed in the segregated dorsal and ventral visual pathways, respectively (*4*).

Six participants (three male and three female, age range 25 to 36) had to learn and recall the association between 10 simple line drawings of real-world objects and 10 locations on a screen during fMRI (*8*). Each learning trial consisted of four conditions, encoding (ENC), control-1 (CO1), retrieval (RET), and control-2 (CO2) (*9*) (Fig. 1A). The behavioral data acquired during RET demonstrated that all six individuals were able to learn the association between object identity and spatial location for all 10 objects within eight learning trials, as indicated by the ensuing asymptotic learning curves (Fig. 2A) (*10*).

Regionally specific changes in evoked responses over time were assessed by examining time-by-condition interactions (*11*). Decreases in activation during learning, indicative of repetition suppression, were observed in several cortical regions in the ventral and dorsal visual pathway (Fig. 2, B and C). Within the framework of repetition suppression it has been hypothesized that decreases in neural responses are epiphenomena of enhanced response selectivity (*5*). By analogy to the development and plasticity of cortical architectures (*12*), this refined selectivity is likely to be due to changes in effective connectivity within the system at a synaptic level. In this study we explicitly addressed this idea by characterizing time-dependent changes in effective connectivity during learning.

Path analysis was used to assess changes in effective connectivity between the dorsal and ventral pathways over time. This technique can be considered as a decomposition of interregional correlations, constrained by an underlying anatomical model. The resulting path coefficients are estimates of effective connectivity and represent the response, in units of standard deviation, of the dependent variable (activity in the target region) for a change of one standard deviation of the explanatory variable (activity in the source region), while activity elsewhere is held constant.

The regions of interest for the path analysis were selected from individual participant analyses of evoked responses (*13*). As expected for visual stimuli consisting of line drawings, we observed responses in striate (V1) and dorsal extrastriate (DE) visual cortex, posterior parietal cortex (PP), and lateral parietal cortex (LP). Ventrally, we found activation of posterior inferotemporal cortex (ITp) and, more anteriorly, in the parahippocampal gyrus (ITa) (Fig. 1B) (*14*).

Given our hypothesis regarding changes in effective connectivity between dorsal and ventral pathways, the path analysis was focused on the connection between PP (dorsal stream) and ITp (ventral stream). We tested changes in this path coefficient, over time within a session, by dividing each learning session into "Early" (first part) and "Late" observations (second part) and estimating separate path coefficients for each (Fig. 1A) (*15*).

The structural model used in our analysis embodies connections within and across ventral and dorsal pathways (Fig. 1B) and is based on anatomical studies in primates (*16*).

The Wellcome Department of Cognitive Neurology, Institute of Neurology, 12 Queen Square, London WC1N 3BG, UK.

*To whom correspondence should be addressed. E-mail: c.buechel@fil.ion.ucl.ac.uk

The right hemisphere plays a predominant role in object-location memory (*1, 17*). We therefore concentrated on the right hemispheric network. Primary visual cortex was modeled as the origin of both pathways. In addition to "interstream" connections between DE and the fusiform region (ITp) and between PP and ITp (*18*), we included direct connections based on hierarchical cortical organization (*16*).

The path coefficient between PP and ITp increased significantly [$\chi^2_{diff}(1) = 13.7$, $P < 0.05$] during learning. This group result was confirmed by the analysis of individual participants that showed an increase in effective connectivity between PP and ITp in all participants (*19*). In contrast to the connections between streams, connections within the dorsal pathway decreased over time. This decrease was significant only for the connection from V1 to DE ($P < 0.05$).

A specious reason for increased path coefficients over time is a learning-related reproducibility of evoked responses in both pathways that is mediated by intraregional mechanisms (that is, repetition suppression as a result of synaptic changes involving only intrinsic connectivity). This explanation can be discounted because within-stream path coefficients should therefore increase. Our data indicate the opposite, namely, that all within-stream connections exhibit only minor changes (decreases) over time. Spurious correla-

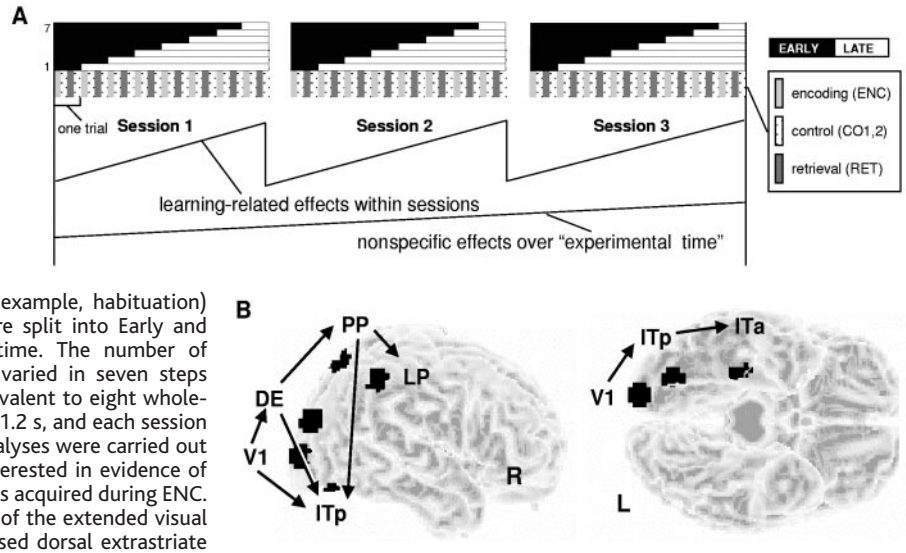

Fig. 1. (**A**) Schematic of the object-location memory experiment. Participants were exposed to three different sets of objects and locations during three consecutive sessions (one set per session). Ten different objects and positions were chosen for each session to minimize carry-over effects (for example, proactive interference) between sessions (*23*). Participants were given eight trials per session in which to learn the associations between object identity and spatial location. The order of the conditions was identical for all eight trials. Using three learning sessions we were able to distinguish between nonspecific time effects (for example, habituation) and learning-related effects. Learning sessions were split into Early and Late to contrast learning-related changes over time. The number of learning trials assigned to Early versus Late was varied in seven steps (horizontal bars). Each condition lasted 32.8 s (equivalent to eight whole-brain fMRI volume acquisitions), each trial lasted 131.2 s, and each session lasted 17.5 min. Image processing and statistical analyses were carried out with SPM97 (*24*). In this analysis, we were only interested in evidence of learning; therefore, the analyses focused on the scans acquired during ENC. (**B**) Effective connectivity was assessed for a model of the extended visual system. In the dorsal pathway, this system comprised dorsal extrastriate cortex (DE), posterior parietal cortex (PP), and a lateral parietal region (LP). Ventrally the system included posterior inferior temporal cortex (ITp) and anterior inferior temporal cortex (ITa). The left panel shows the brain from the right; the right panel shows the inferior surface of the brain, with the cerebellum removed to reveal inferior temporal cortex. Black patches show the regions of interest and their location in a single participant. Connections are in accord with a hierarchical organization of the visual system (*16*). We were mainly interested in the connection between PP and ITp, given our hypothesis that effective connectivity would increase between regions over time.

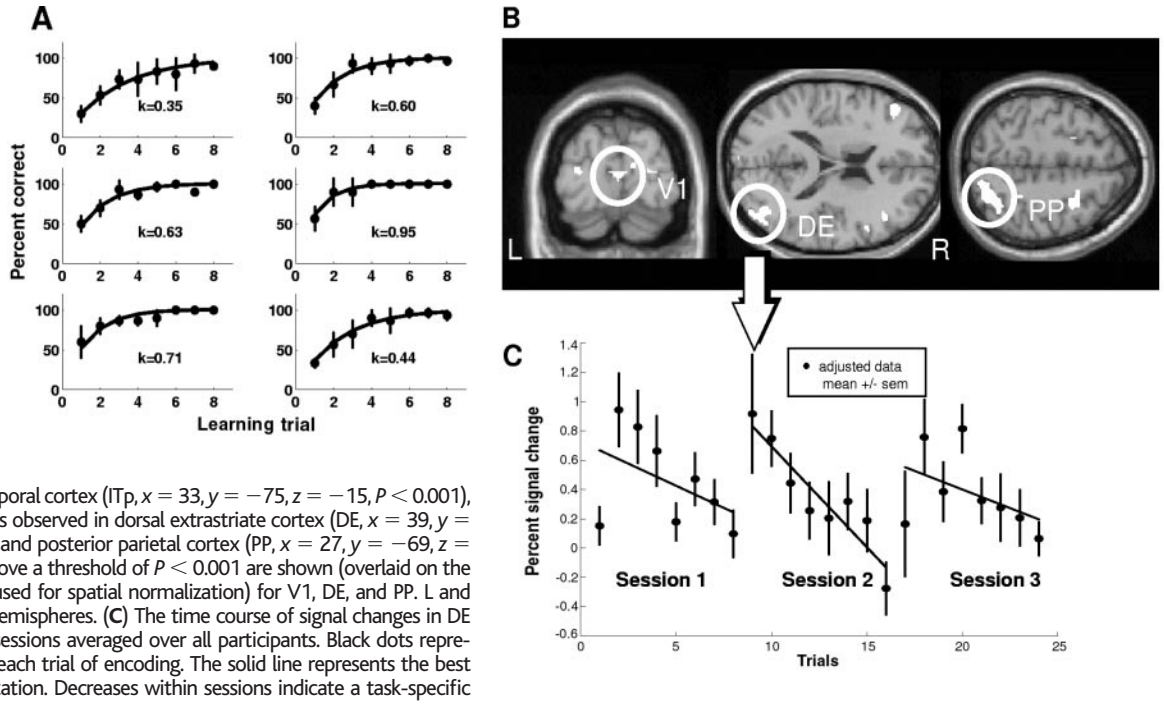

Fig. 2. (**A**) Averaged learning curves (mean ± SEM) for all six participants for three learning sessions. The performance was well approximated by the function $1 - e^{-kx}$. The parameter k is a metric of learning speed, where small values of k indicate slow learning. (**B**) As predicted, cortical regions showed adaptation of responses over time, indicative of repetition suppression (*5*). In addition to primary visual cortex (V1, $x = 3, y = -90, z = 9$, $P < 0.001$) and inferotemporal cortex (ITp, $x = 33, y = -75, z = -15$, $P < 0.001$), repetition suppression was observed in dorsal extrastriate cortex (DE, $x = 39, y = -72, z = 18$, $P < 0.001$) and posterior parietal cortex (PP, $x = 27, y = -69, z = 54$, $P < 0.001$). Voxels above a threshold of $P < 0.001$ are shown (overlaid on the structural MRI template used for spatial normalization) for V1, DE, and PP. L and R indicate left and right hemispheres. (**C**) The time course of signal changes in DE during all three learning sessions averaged over all participants. Black dots represent the mean signal for each trial of encoding. The solid line represents the best linear fit, indicating adaptation. Decreases within sessions indicate a task-specific effect.

tions between PP and ITp could be caused by a common input (V1). However, path analysis (that is, effective connectivity) as used here explicitly takes common inputs into account and is able to dissociate these nonspecific effects from interactions between PP and ITp.

Although dorsal visual regions may exert more influence on ventral areas (*20*), knowledge about the preferred direction of those interstream connections is sparse. Initially, interstream connections were modeled from dorsal to ventral areas. Nevertheless, we ensured the robustness of our findings by reversing these connections, with no significant change in fit [$\chi^2_{diff}(1) = 10.3$, $P < 0.05$]. There is no evidence in our data that allows inferences about the direction of this connection (a sufficient model is obtained with either direction). This is entirely consistent with reciprocal projections and interactions between the two areas, which, of course, is the most biologically plausible situation.

To ensure that increases in effective connectivity were specific to encoding or learning, we also tested for changes in effective connectivity during the control conditions. No significant differences [$\chi^2_{diff}(1) = 0.1$, $P = 0.9$ for both control conditions] between Early and Late were found. Applying the same analysis to the retrieval condition did not show a significant increase over time [$\chi^2_{diff}(1) = 0.2$, $P = 0.7$]. If present, temporal changes in effective connectivity between ITp and PP during retrieval were probably obscured by the stimulus-driven activation of ITp by the visual cue (nonsense shape) presented during retrieval. ITp neurons responding to visual features of the cue do not contribute to the concerted activation of neuronal populations involved in associative learning because they are not associated with a specific location.

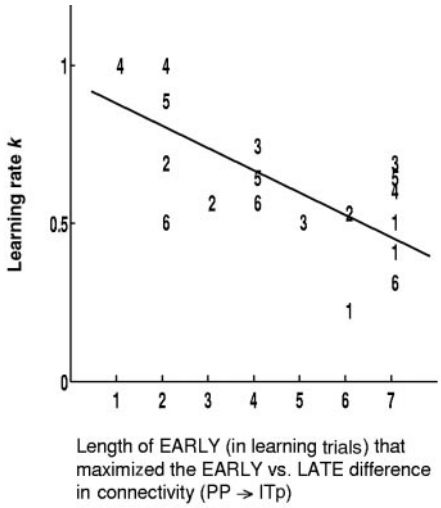

Fig. 3. Varying the cut-off between Early and Late determined the estimate of change in the PP-to-ITp connection. We determined the cut-off time for each participant and session that maximized this difference in connectivity. This value strongly predicted [$F(2,15) = 6.6$, $P < 0.05$] the behaviorally determined learning speed (k). Intuitively, this means that for fast learning the biggest change in PP-to-ITp connectivity is attained earlier in the learning session.

The estimated change in connectivity from PP to ITp clearly depends on the cut-off point between Early and Late. To unequivocally establish a relation between neurophysiologically mediated changes in connectivity and behavioral learning, we examined the relation between the temporal pattern of effective connectivity changes and learning speed for all sessions and participants. We estimated the differences in effective connectivity for seven Early and Late partitions by successively shifting the cut-off (all seven cut-offs are shown as horizontal bar graphs in Fig. 1A). The cut-off time at which the connectivity change peaked was used as a temporal index of changes in effective connectivity (that is, plasticity) (*21*). The significant regression [$F(2,15) = 6.6$, $P < 0.05$; Fig. 3] of k, a measure of learning speed, on this plasticity index indicated that for fast learning (high values of k) the maximum difference in path coefficients between PP and ITp was achieved earlier in the session (that is, Early comprises less scans relative to Late). In other words, the temporal pattern of changes in effective connectivity strongly predicted learning performance.

In summary, our data are in accord with the concept of repetition suppression: the adaptation of regional neural responses over multiple repetitions. Moreover, our data directly support the hypothesis that repetition suppression is paralleled by changes in the functional integration of the dynamic cell assemblies that express it. As responses within an area decrease with learning, effective connectivity between cortical areas increases. The correlation between speed of learning and these changes in effective connectivity emphasize the relevance of plastic changes in functional integration for associative learning.

References and Notes

1. B. Milner, I. Johnsrude, J. Crane, *Philos. Trans. R. Soc. London Ser. B* **352**, 1469 (1997).
2. C. Moscovitch, S. Kapur, S. Kohler, S. Houle, *Proc. Natl. Acad. Sci. U.S.A.* **92**, 3721 (1995).
3. S. Kohler *et al*., *Neuropsychologia* **36**, 129 (1998); A. M. Owen, B. Milner, M. Petrides, A. C. Evans, *J. Cognit. Neurosci.* **8**, 588 (1996).
4. L. G. Ungerleider and J. V. Haxby, *Curr. Opin. Neurobiol.* **4**, 157 (1994); M. Mishkin, L. G. Ungerleider, K. A. Macko, *Trends Neurosci.* **6**, 414 (1983).
5. R. Desimone, *Proc. Natl. Acad. Sci. U.S.A.* **93**, 13494 (1996); C. L. Wiggs and A. Martin, *Curr. Opin. Neurobiol.* **8**, 227 (1998). Repetition suppression is mainly observed in inferior temporal cortex [G. C. Baylis and E. T. Rolls, *Exp. Brain Res.* **65**, 614 (1987)], but it has also been observed in other regions, including parietal cortex [L. R. Squire *et al*., *Proc. Natl. Acad. Sci. U.S.A.* **89**, 1837 (1992); R. L. Buckner *et al*., *J. Neurosci.* **15**, 12 (1995); D. L. Schacter *et al*., *Proc. Natl. Acad. Sci. U.S.A.* **93**, 321 (1996)].
6. M. M. Mesulam, *Ann. Neurol.* **28**, 597 (1990); A. R. Damasio and H. Damasio, in *Large Scale Neuronal Theories of the Brain*, C. Koch and J. L. Davis, Eds. (MIT Press, Cambridge, MA, 1994).
7. For the origins of the concept of effective connectivity, see G. L. Gerstein and D. H. Perkel, *Science* **164**, 828 (1969); A. Aertsen and H. Preissl, *Dynamics of Activity and Connectivity in Physiological Neuronal Networks* (VCH, New York, 1991). For examples of the adaptation to functional neuroimaging, see K. J. Friston, L. G. Ungerleider, P. Jezzard, R. Turner, *Hum. Brain Mapp.* **2**, 211 (1995); B. Horwitz *et al*., *J. Cognit. Neurosci.* **4**, 311 (1992); A. R. McIntosh and F. Gonzalez-Lima, *Hum. Brain Mapp.* **2**, 2 (1994). For a recent example of the application of the concept in the context of learning, see A. R. McIntosh, R. E. Cabeza, N. J. Lobaugh, *J. Neurophysiol.* **80**, 2790 (1998).
8. Informed consent was obtained before MRI scanning. Data were acquired with a 2 Tesla Magnetom VISION (Siemens, Erlangen, Germany) whole-body MRI system equipped with a head volume coil. We obtained contiguous multislice T2*-weighted fMRI images [echo time (TE) = 40 ms; 80.7 ms per image; 64 by 64 pixels (19.2 cm by 19.2 cm)] with echo-planar imaging using an axial slice orientation. A T2*-weighted sequence was chosen to enhance blood oxygenation level–dependent contrast. The volume acquired covered the whole brain (48 slices, each 3 mm thick, 4.1 s per volume).
9. Each object was taken from a standardized series [J. G. Snodgrass and M. Vanderwart, *J. Exp. Psychol. Hum. Learn.* **6**, 174 (1980)] and subtended 4° by 4° visual angle (visible screen 22° by 17°). Participants were familiarized with the objects before each learning session. During ENC each of 10 line drawings was presented sequentially (the order was randomized over all eight repetitions) for 2.5 s in its location. Locations were indicated by boxes visible throughout the condition. A new object was presented every 3.2 s. The task was to name the object. All objects had monosyllabic names, allowing participants to utter the object name without jaw or head movements (estimated head motion <1.5 mm). Participants' vocal responses were recorded by a differential microphone set-up. During RET participants were spatially cued with a nonsense shape and had to respond with the name of the object previously associated with that location. Stimulus timing was identical in all conditions.
10. All individual learning curves were well approximated by the function $1 - e^{-kx}$, where $0 < k < 1$ is an index of learning speed. Small values of k indicate a flatter curve and therefore slower learning.
11. The four original box-car functions were multiplied by a monotonically increasing linear function, leading to four additional regressors, which model time-by-condition interactions. [C. Büchel, J. Morris, R. J. Dolan, K. J. Friston, *Neuron* **20**, 947 (1998)].
12. W. Singer, *Science* **270**, 758 (1995).
13. Regions of interest (ROIs) were based on the SPM{F}. The time series, representative of a region, was defined by the first eigenvector of all voxel time series in an ROI, centered (8-mm radius) around the local F maximum (*22*). Time series were adjusted for confounds (for example, global mean, low-frequency components and head motion).
14. Activation at the calcarine fissure was assigned to V1 (mean ± SEM in millimeters for all participants: $x = 8 \pm 3.4$, $y = -88 \pm 2$, $z = 0.5 \pm 2$). DE activation was found close to area V3a ($x = 30 \pm 2.1$, $y = -86.5 \pm 1.8$, $z = 20.7 \pm 1.5$) [R. B. H. Tootell *et al*., *J. Neurosci.* **17**, 7060 (1997)]. The locations of PP ($x = 25 \pm 3.1$, $y = -63.5 \pm 2.8$, $z = 57.5 \pm 2.4$) and LP ($x = 38 \pm 2.5$, $y = -42 \pm 3.3$, $z = 54 \pm 2.3$) were similar to previous neuroimaging studies [(*2*); B. Luna *et al*., *Cereb. Cortex* **8**, 40 (1998)]. The location of the posterior ventral extrastriate region was found in the fusiform gyrus (ITp) ($x = 34.5 \pm 4$, $y = -68 \pm 3.4$, $z = -17 \pm 1.3$); the more anterior ventral activation was in the parahippocampal gyrus (ITa) ($x = 33.5 \pm 0.9$, $y =$

-34.5 ± 1.3, $z = -24 \pm 2.3$). Coordinates for these regions were comparable to previous studies (*1*).

15. Path coefficients for Early and Late were estimated with a maximum likelihood function implemented in MatLab (Mathworks, Natick, MA). The operational equations have been reported elsewhere (*22*). The covariance matrices used were calculated on the basis of observations during ENC for Early and Late (Fig. 1A). Two stacked models were compared to assess the significance of changes over time: a free model in which all paths other than the path from PP to ITp were forced to be equal for Early and Late, and a restricted model in which all path coefficients were constrained to be the same for Early and Late. This allowed us to test for differences in fit as a function of one path coefficient (PP to ITp). We analyzed the group as a whole and each participant individually. In the context of multivariate normally distributed variables, the minimum of the maximum likelihood function times the number of observations minus 1 has a χ^2 distribution with $(q/2) \times (q + 1) - p$ degrees of freedom [K. A. Bollen, *Structural Equations with Latent Variables* (Wiley, New York, 1989)], where p is the number of free parameters and q is the number of observed variables. The significance of the difference between models is expressed by the difference in the χ^2 goodness of fit. This χ^2 statistic has n degrees of freedom, where n is the difference in the degrees of freedom between the null model and the one in question.
16. D. J. Felleman and D. C. Van Essen, *Cereb. Cortex* **1**, 1 (1991).
17. M. L. Smith and B. Milner, *Neuropsychologia* **19**, 781 (1981); S. Kohler, A. R. McIntosh, M. Moscovitch, G. Winocur, *Cereb. Cortex* **8**, 451 (1998).
18. C. Distler, D. Boussaoud, R. Desimone, L. G. Ungerleider, *J. Comp. Neurol.* **334**, 125 (1993).
19. Mean changes in path coefficients for all three sessions between Early and Late for participants 1 to 6 were calculated using a correlation matrix based on 96 observations during ENC for Early and 96 observations during ENC for Late: 0.27*, 0.21, 0.37*, 0.24*, 0.19, 0.31* (*$P < 0.05$). The group effect was tested by stacking these 96 observations for all six participants, leading to 576 observations for each correlation matrix. Confounding participant and session effects were partialled out by least squares. The group analysis for the left hemisphere showed only a trend [$\chi^2_{diff}(1) = 2.3$, $P = 0.13$]. To account for autocorrelation in the observations, we used the effective degrees of freedom in the calculation of all fit indices [K. J. Worsley and K. J. Friston, *Neuroimage* **2**, 173 (1995)].
20. B. Jouve, P. Rosenstiehl, M. Imbert, *Cereb. Cortex* **8**, 28 (1998).
21. The length of Early was varied in seven steps including the first 32, 64, 96, 128, 160, 192, and 224 out of a total of 256 scans for each session (Fig. 1A). The difference for the path coefficient for PP to ITp was calculated for each cut-off in all three sessions for all participants. The peak of the difference [that is, the cutoff (1 to 7)] that maximized the difference between Early and Late is an index of the temporal pattern of changes in effective connectivity. The learning speed parameter k (range 0 to 1), obtained from fitting $1 - e^{-kx}$ to the behavioral data (the percent of correct responses) was regressed on peak cut-off. Between-participant and between-session effects were modeled separately and both reached significance [$t(15) = 3$, $t(15) = 2.1$, $P < 0.05$]. Intuitively this result indicates that the temporal pattern of changes in effective connectivity not only predicted a given participant's performance but also differences in learning between sessions for an individual participant.
22. C. Büchel and K. J. Friston, *Cereb. Cortex* **7**, 768 (1997).
23. The interpretation of changes over time in learning experiments can be difficult due to nonspecific time effects (that is, habituation, motivation, and arousal). We dissociated learning-related effects from nonspecific time effects by using three sequential learning sessions. Nonspecific time effects unrelated to learning are expressed over the duration of the whole "experimental time" (that is, over all three sessions). Conversely, learning-related effects should follow a similar pattern, but within each learning session (Figs. 1A and 2C).
24. K. J. Friston, A. P. Holmes, J. Ashburner, J.-B. Poline, "SPM Central," available at http://www.fil.ion.ucl.ac.uk/spm; K. J. Friston *et al*., *Hum. Brain Mapp.* **2**, 189 (1995). All volumes were realigned to the first volume. A structural MRI, acquired with a standard three-dimensional T1-weighted sequence (1 mm by 1 mm by 1.5 mm voxel size), was coregistered to the T2* images. Finally, all the images were spatially normalized [K. J. Friston *et al*., *Hum. Brain Mapp.* **2**, 1 (1995)] to a standard template [A. C. Evans *et al*., in proceedings of the *Nuclear Science Symposium and Medical Imaging Conference*, L. A. Klaisner, Ed., San Francisco, CA, 31 October to 6 November, 1993 (IEEE Service Center, Piscatawa, NJ, 1993), vols. 1–3, pp. 1813-1817]. The data were spatially smoothed with a 6-mm full width at half maximum (FWHM) Gaussian kernel. Data analysis was performed by modeling the different conditions (ENC, CO1, RET, and CO2) as reference waveforms (that is, box-cars convolved with a hemodynamic response function) in the context of multiple linear regression. The resulting F statistics for every voxel constitute a statistical parametric map SPM{F}. Data were analyzed for each participant individually with a threshold of $P < 0.05$ (corrected for multiple comparisons). An adaptive highpass filter was added to the confound partition of the design matrix to account for low-frequency drifts [A. P. Holmes, O. Josephs, C. Büchel, K. J. Friston, *Neuroimage* **5**, S480 (1997)]. Voxel time series were temporally smoothed with a Gaussian filter (FWHM of 4 s).
25. We thank the departmental radiographers and the Functional Imaging Laboratory physics group for help with fMRI scanning, O. Josephs for the development of the sound pickup system in fMRI, and A. Kleinschmidt, I. Johnsrude, R. Frackowiak, and R. Henson for invaluable discussions. C.B., J.T.C., and K.J.F. were supported by the Wellcome Trust.

29 October 1998; accepted 2 February 1999

Cytokinin Activation of *Arabidopsis* Cell Division Through a D-Type Cyclin

Catherine Riou-Khamlichi,[1]* Rachael Huntley,[1] Annie Jacqmard,[2] James A.H. Murray[1]†

Cytokinins are plant hormones that regulate plant cell division. The D-type cyclin CycD3 was found to be elevated in a mutant of *Arabidopsis* with a high level of cytokinin and to be rapidly induced by cytokinin application in both cell cultures and whole plants. Constitutive expression of CycD3 in transgenic plants allowed induction and maintenance of cell division in the absence of exogenous cytokinin. Results suggest that cytokinin activates *Arabidopsis* cell division through induction of CycD3 at the G_1-S cell cycle phase transition.

Cytokinins are purine derivatives that promote and maintain plant cell division in cultures (*1*–*8*) and are also involved in various differentiation processes including shoot formation, photomorphogenesis, and senescence (*2*, *3*). In promoting cell division, cytokinins act synergistically with auxins (*3*, *4*).

Because restimulation of quiescent vertebrate cells into division by mitogenic signals requires the transcriptional up-regulation of D-type cyclins (*9*), the existence of related proteins in plants (*10*, *11*) suggests plant D-type cyclins (CycD) as potential mediators of plant mitogenic signals. A possible role for cytokinin in regulating the expression of the *Arabidopsis CycD3* gene in callus material (*10*) was investigated in a dispersed suspension culture of *Arabidopsis* cells (*12*, *13*).

Cells incubated for 24 hours without hormones (*14*) accumulated CycD3 transcripts in response to cytokinin supplied at concentrations down to 10^{-3} μM (Fig. 1, A and B), starting within 1 hour (Fig. 1C). Zeatin, the most abundant cytokinin in *Arabidopsis* (*15*), and 6-benzylaminopurine (BAP) generated the strongest response, whereas adenine, a purine lacking cytokinin properties, showed no effect (Fig. 1A).

CycD3 induction could be a direct response to cytokinin or an indirect response caused by cells reaching a certain cell cycle position under the influence of cytokinin. Cycloheximide (Chx) blocks both G_1 phase progression (*13*) and protein synthesis in these cells (*14*) and did not inhibit CycD3 induction by cytokinin (Fig. 1D), showing that induction is independent of progression through G_1 and involves signal transduction by proteins already present in stationary phase cells. Inhibition of CycD3 induction by the protein phosphatase inhibitor okadaic acid and gratuitous induction by the protein kinase inhibitor staurosporine in the absence of cytokinin (Fig. 1, E and F) implicate regulatory phosphorylations in this process.

Whole plant responses to hormones are complex (*2*, *3*) and do not necessarily reflect

[1]Institute of Biotechnology, University of Cambridge, Tennis Court Road, Cambridge CB2 1QT, UK. [2]Département de Biologie Végétale, Université de Liège, Service de Physiologie, Sart Tilman, B4000 Liège, Belgium.

*Present address: Faculté des Sciences, Institut de Biotechnologie, Université de Limoges, 123 avenue Albert Thomas, 87060 Limoges, France.
†To whom correspondence should be addressed. E-mail: j.murray@biotech.cam.ac.uk